

PAPER

Coordination polymers of alkali metal trithiocyanurates: structure determinations and ionic conductivity measurements using single crystals†

Cite this: *CrystEngComm*, 2013, 15, 9400

Satoshi Tominaka,^{*ab} Sebastian Henke^b and Anthony K. Cheetham^{*b}

Six novel crystalline coordination polymers composed of alkali metal ions and trithiocyanurate anions ($C_3N_3S_3H_2^- = \text{ttcH}_2^-$) were synthesized. Single crystals were used both for structure determinations by X-ray diffraction and ionic conductivity measurements by AC impedance methods. The structures are: (i) sodium trithiocyanurate trihydrate, $\text{Na}(\text{ttcH}_2)(\text{H}_2\text{O})_3$ in space group $P2_1$; (ii) potassium trithiocyanurate hydrate, $\text{K}(\text{ttcH}_2)(\text{H}_2\text{O})$ in $P\bar{1}$; (iii) rubidium trithiocyanurate hydrate, $\text{Rb}(\text{ttcH}_2)(\text{H}_2\text{O})$ in $P\bar{1}$; (iv) rubidium trithiocyanurate hydrate, $\text{Rb}_3(\text{ttcH}_2)_2(\text{ttcH}_3)_2(\text{H}_2\text{O})_5(\text{OH})$ in $P\bar{1}$; and (v, vi) two anhydrous polymorphs of caesium trithiocyanurates, $\text{Cs}(\text{ttcH}_2)$ in $P\bar{1}$ and Cc . With the exception of the sodium phase, which is layered, all of these compounds consist of three dimensional coordination networks. In all systems, the inorganic regions are interleaved by arrays of ttcH_2^- anions. The most interesting feature of this system is the thiol-rich environment formed between the trithiocyanurate layers, where alkali metal ions are located. Water molecules, where present, are always coordinated to a cation. Among these crystals, $\text{K}(\text{ttcH}_2)(\text{H}_2\text{O})$ exhibited proton conductivity under atmospheric conditions (25 ± 0.2 °C): $1.1 \times 10^{-5} \text{ S cm}^{-1}$ in the direction perpendicular to the bc plane and $3.1 \times 10^{-6} \text{ S cm}^{-1}$ along the c axis.

Received 15th June 2013,
Accepted 16th July 2013

DOI: 10.1039/c3ce41150h

www.rsc.org/crystengcomm

1 Introduction

There is an increasing demand for advanced solid-state ion conductors for batteries, fuel cells, and sensors. A variety of materials, including oxides, nitrides, sulfides and polymers, have been synthesized and investigated as ion conductors.^{1,2} Inorganic–organic hybrid systems have been attracting interest during the past decade, especially in areas such as catalysis, ion exchange, and gas storage. Hybrid materials are generally composed of cations, such as transition metal ions, and anionic organic ligands, such as carboxylates; compared with classical inorganic materials, they have much greater structural and chemical diversity.³ A major research effort has been focused on porous frameworks of these hybrid systems. However, dense structures, which do not have solvent-accessible pores and are more similar to classical inorganic materials, are attracting attention on account of their exciting

magnetic, optical, and electronic properties.^{4–8} Regarding ionic conductor applications, porous coordination polymers have been used as host frameworks to achieve fast ionic transport through guest molecules,^{9–11} but little has been reported on ionic conduction of either protons or lithium ions in dense hybrid system.^{12,13}

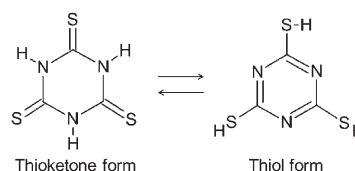
Compared with classical solid-state materials, dense hybrid materials generally have less-packed structures associated with the geometric constraints of organic molecules, suggesting a good prospect for ionic transport. In order to enable cation diffusion in dense systems, coordination sites formed by heteroatoms (*e.g.*, O, N and S) and π electrons are necessary, but aliphatic groups seem to hinder ionic transport. Among hetero atoms, the greater polarizability of the sulfur groups is of great importance to achieve excellent conductivity, though this feature in turn leads to decreased thermal stability.

^a International Center for Materials Nanoarchitectonics (WPI-MANA), National Institute for Materials Science (NIMS), Ibaraki 305-0044, Japan.

E-mail: TOMINAKA.Satoshi@nims.go.jp; Tel: +81 (0)29 860 4594

^b Department of Materials Science and Metallurgy, University of Cambridge, Pembroke Street, Cambridge CB2 3QZ, UK. E-mail: akc30@cam.ac.uk; http://www.msm.cam.ac.uk/fihm/; Fax: +44 (0)1223 334567; Tel: +44 (0)1223 767061

† Electronic supplementary information (ESI) available: thermogravimetric analyses, powder XRD patterns and FTIR spectra. CCDC 944676–944682. For ESI and crystallographic data in CIF or other electronic format see DOI: 10.1039/c3ce41150h



Scheme 1 Trithiocyanuric acid.

In this scenario, we have focused on trithiocyanuric acid (TTCA = ttcH_3 , Scheme 1) as a versatile ligand (*i.e.*, anions) for the construction of dense hybrid frameworks.

This molecule has been used in industry, *e.g.*, for the removal of heavy metal ions from waste, production of composite materials with metals and polymers, and electroplating of silver and nickel.¹⁴ Most of the reported crystal structures of TTCA-based coordination polymers were composed of divalent cations.^{14,15} TTCA is a weak acid ($\text{p}K_{\text{a}1} = 5.71$, $\text{p}K_{\text{a}2} = 8.36$ and $\text{p}K_{\text{a}3} = 11.38$)¹⁵ comparable to acetic acid, and is known to form molecular crystals through hydrogen bonding.^{16,17} Notice, that in the solid state the thioketone form is significantly more stable than the thiol form (Scheme 1).

Since the influence of grain boundaries and particle surfaces is significant in solid-state ion conductors,^{18,19} we used single crystal samples for both the structure analysis and the impedance measurements in order to develop a better understanding of the relationship between crystal structure and conductivity. For this purpose, we developed a new setup for single-crystal AC impedance measurements (Fig. 1).

Here we report the synthesis and structures of several alkali metal trithiocyanurates as well as their ionic conductivities.

2 Experimental

2.1 Synthesis

Dense hybrid crystals of TTCA-based coordination polymers were synthesized from TTCA (Sigma-Aldrich) and alkali metal salts, sodium acetate (NaOOCCH_3 , Fisher), potassium carbonate (K_2CO_3 , Fisher), rubidium nitrate (RbNO_3 , Alfa Aesar), and caesium nitrate (CsNO_3 , Alfa Aesar). Lithium hydroxide (LiOH , Fisher) was used as a deprotonation agent. The crystals

were formed by dissolving TTCA and the respective metal salt in distilled water at 90 °C followed by crystal growth from the mother solution at room temperature. The crystals were recovered by filtration under reduced pressure, rinsed with ethanol and chloroform, and then dried in air. More details are described in the ESI† file.

2.2 Structure determinations

The crystal structure was determined by single crystal diffraction using an Oxford Diffraction Gemini A Ultra X-ray diffractometer with Cu $K\alpha$ radiation ($\lambda = 1.54184 \text{ \AA}$) operated at 40 kV and 40 mA. Data were collected under atmospheric conditions ($\sim 300 \text{ K}$), except for the Cs compounds, which have been measured at 300 K under nitrogen flow, and the Na compound, which has been measured at both 120 K under nitrogen flow and at ambient conditions. Data collection, unit cell determination and refinement, absorption correction and data reduction were performed using the CrysAlisPro software from Agilent Technologies. An analytical absorption correction was performed by applying a face-based absorption correction as well as a spherical absorption correction.

The structures were solved by direct methods and were then refined by the least squares methods using the SHELX program²⁰ within the Olex2 interface.²¹ All non-hydrogen atoms were refined anisotropically and hydrogen atoms were refined isotropically. Hydrogen atoms on trithiocyanurate molecules were then added to calculated positions. Those on water molecules were added to chemically reasonable positions found in the Fourier difference map, and then refined with constrained O–H distances (0.958 Å) and H–O–H angles (104.5°) taken from the water molecule.²² Some of the hydrogen atoms were refined only with the O–H distance constraint (see Fig. 2c).

Visualization of structures was carried out using the VESTA program.²³ Details of crystal information, including bond lengths, is available in the ESI† CIF files are available for the structures described herein.‡

2.3 Conductivity measurements

Conductivities of single crystals were measured by the AC impedance method using an electrochemical instrument (Gamry Interface 1000) in the frequency range of 1 MHz to 1 Hz at an AC amplitude of 100 mV in air or nitrogen. The crystals were physically contacted with Au microelectrodes (200 nm thick) deposited on a SiO_2 chip. Two Au microelectrodes designed to have a 80 μm gap (Fig. 1) were prepared on SiO_2 by photolithography through the previously reported procedure.²⁴ This size is nearly the same as the size of the single crystals used for structure determination *via* X-ray diffraction.

Using pressure sensitive silicone adhesive polyimide film (CMF-100-020W from MicroNova, $-70 \text{ }^\circ\text{C}$ to $+260 \text{ }^\circ\text{C}$), crystals were gently picked up and mounted on the electrodes as

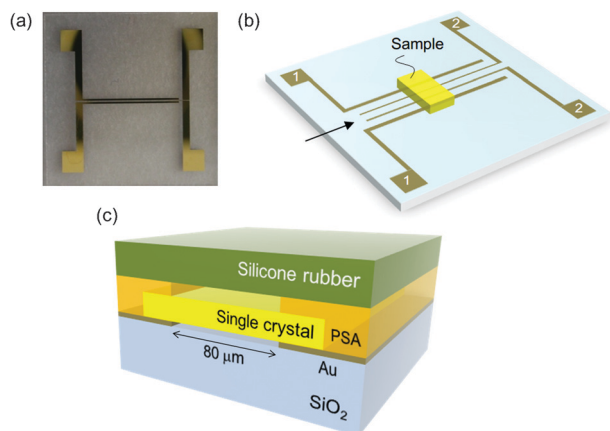


Fig. 1 Schematic illustration of the setup for single crystal AC impedance measurements. (a) Picture of the Au microelectrodes on a SiO_2 substrate (1 cm \times 1 cm, 0.5 mm thick). (b) Schematic for illustrating the overall design. A single crystal sample is placed on the central part where four lines are located. Electrodes '1' are 100 μm wide and are used for AC impedance measurements. Electrodes '2' are 10 μm wide and are used for four-probe measurements (not used in this work). The gaps between electrodes are 20 μm . (c) Cross-sectional image along the arrow shown in panel 'b'. The single crystal sample is fixed by pressure sensitive adhesive, PSA, and gently pressed with a silicone rubber.

‡ CCDC 944676–944682 contain the supplementary crystallographic data for this paper.

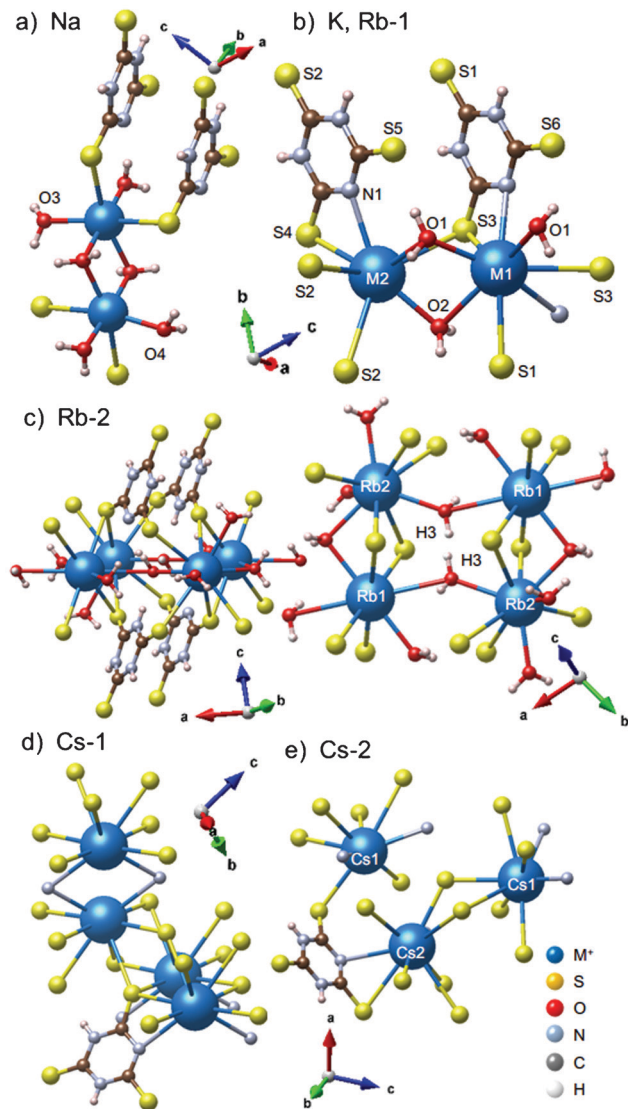


Fig. 2 Comparison of connectivity of trithiocyanurate with alkali metal ions. (a) Na-TTC. O3 and O4 are independent. (b) K-TTC and Rb-TTC-1. (c) Rb-TTC-2. Occupancy of H3 is 0.5. These hydrogen atoms and those on the same O atoms were refined without the angle constraint. (d) Cs-TTC-1. (e) Cs-TTC-2.

illustrated in Fig. 1c. In order to check anisotropy in the conductivities, crystallographic orientations were checked using X-ray diffraction, and then crystals were aligned on the chip under an optical microscope.

The temperature was controlled using a Supercool PR-59 temperature control module, a thermoelectric module placed on the back side of the SiO₂ substrate and a negative temperature coefficient thermistor (10 kΩ at 25 °C, Epcos B57861S0103F45) contacted with the front side of the substrate.

In order to verify this measurement, especially contact between electrodes and crystal faces, a crystal of the known charge-transfer complex, tetrathiafulvalene nitrate, was synthesized and its single crystal AC impedance measurement was tested. As a result, a semicircle behaviour, which is assignable to electron conduction, was obtained. Thus, we judged that this measurement setup is highly reliable.

2.4 Other analyses

Thermogravimetric analysis and differential scanning calorimetry were performed simultaneously using a TA Instruments Q600 SDT instrument with a nitrogen gas flow of 100 mL min⁻¹ at a heating rate of 5 °C min⁻¹, from room temperature to 600 °C. It was found that trithiocyanuric acid itself decomposed endothermically around 300 °C (Fig. S1, ESI†). The alkali metal trithiocyanurates show similar decomposition temperatures suggesting that the ligand decomposition determines the overall thermal stability of these frameworks.

Powder X-ray diffraction (PXRD) was carried out using a Bruker-AXS D8 diffractometer with Cu Kα radiation ($\lambda = 1.5418 \text{ \AA}$) and a LynxEye position sensitive detector in the Bragg-Brentano geometry. The samples were prepared by grinding the crystals gently using mortar and pestle for 1 min. Data were collected in the 2θ range of 5–60° at room temperature. Most of the compounds are confirmed to be phase pure, except for the polymorphs of the Cs compounds (Fig. S2e, ESI†).

Fourier-transform infrared spectroscopy (FTIR) was carried out using a Bruker Tensor 27 infrared spectrometer with a diamond attenuated total reflectance (ATR) attachment. The samples were prepared by grinding the crystals gently using a mortar and pestle for 1 min. The data were collected in the wavenumber range from 520 to 4000 cm⁻¹ at room temperature. The absorption was normalized relative to the peaks assignable to C=S stretching vibration (1100 to 1160 cm⁻¹)²⁵ and plotted with shifts.

The chemical compositions were determined by CHN elemental analysis (Department of Chemistry, University of Cambridge). Elemental analysis data. Na-TTC: found C, 14.26; H, 2.95; N, 16.52%; calcd for NaC₃H₈O₃N₃S₃ (see Table 1) C, 14.23; H, 3.16; N, 16.59%. K-TTC: found C, 15.41; H, 1.58; N, 17.86%; calcd for KC₃H₄ON₃S₃C, 15.44; H, 1.71; N, 18.01%. Rb-TTC-1: found C, 12.81; H, 1.34; N, 14.88%; calcd for RbC₃H₄ON₃S₃C, 12.88; H, 1.43; N, 15.02%. Rb-TTC-2: found C, 13.51; H, 1.65; N, 15.56%; calcd for Rb₃C₁₂H₂₁O₆N₁₂S₁₂C, 13.47; H, 1.96; N, 15.70%. Cs-TTC-1: found C, 11.64; H, 0.54; N, 13.35%; Cs-TTC-2: found C, 11.63; H, 0.57; N, 13.38%; calcd for CsC₃H₂N₃S₃C, 11.66; H, 0.65; N, 13.59%. These compositions are consistent with those determined by X-ray diffraction. The slight discrepancies in the hydrogen content are attributable to its low concentration, and the errors are within a reasonable range for the CHN analysis.

3 Results and discussion

3.1 Structure of alkali metal trithiocyanurates

Six novel hybrid crystals were obtained. Sodium trithiocyanurate hydrate, referred to as “Na-TTC”, crystallises as clear light yellow rectangular prisms. Potassium trithiocyanurate hydrate, “K-TTC”, and rubidium trithiocyanurate hydrate, “Rb-TTC-1”, form clear colourless rhombohedral crystals. Rubidium trithiocyanurate hydrate, “Rb-TTC-2”, forms clear light yellow rectangular prisms. Caesium trithiocyanurates can be prepared as two different anhydrous polymorphs: “Cs-TTC-1” crystallises

Table 1 Summary of crystal data for alkali metal trithiocyanurates

Compound	Na-TTC	K-TTC	Rb-TTC-1	Rb-TTC-2	Cs-TTC-1	Cs-TTC-2
Formula ^a	Na(ttcH ₂)(H ₂ O) ₃	K(ttcH ₂)(H ₂ O)	Rb(ttcH ₂)(H ₂ O)	Rb ₃ (ttcH ₂) ₂ (ttcH ₃) ₂ (H ₂ O) ₅ (OH)	Cs(ttcH ₂)	Cs(ttcH ₂)
Formula weight/g	253.24	233.35	279.72	1070.41	309.16	309.16
Asymmetric unit	Na ₂ C ₆ H ₁₆ O ₆ N ₆ S ₆	K ₂ C ₆ H ₈ O ₂ N ₆ S ₆	Rb ₂ C ₆ H ₈ O ₂ N ₆ S ₆	Rb _{1.5} C ₆ H _{10.5} O ₃ N ₆ S ₆	CsC ₃ H ₂ N ₃ S ₃	Cs ₂ C ₆ H ₄ N ₆ S ₆
Crystal system	Monoclinic	Triclinic	Triclinic	Triclinic	Triclinic	Monoclinic
Space group	<i>P</i> 2 ₁	<i>P</i> $\bar{1}$	<i>P</i> $\bar{1}$	<i>P</i> $\bar{1}$	<i>P</i> $\bar{1}$	<i>C</i> c
<i>a</i> /Å	10.3697(4)	7.3438(4)	7.3545(3)	7.5673(3)	5.1031(3)	5.41409(8)
<i>b</i> /Å	12.6801(3)	10.3247(4)	10.5336(4)	11.2806(6)	7.9838(6)	21.2829(3)
<i>c</i> /Å	7.7756(2)	11.6813(5)	11.7338(5)	11.4428(4)	10.9408(6)	14.9761(2)
α (°)	90	76.285(3)	76.921(4)	107.984(4)	96.431(5)	90
β (°)	109.059(4)	80.914(4)	80.641(4)	94.103(3)	103.270(5)	92.3402(13)
γ (°)	90	87.551(4)	88.730(4)	102.469(4)	104.265(5)	90
<i>V</i> /Å ³	966.37(5)	849.64(7)	873.54(7)	897.06(7)	413.70(4)	1724.22(4)
<i>Z</i>	2	2	2	2	2	4
<i>R</i> ₁ , <i>wR</i> ₂	2.90%, 7.97%	3.72%, 10.28%	3.25%, 8.85%	2.95%, 7.45%	3.01%, 8.52%	4.60%, 12.07%
GOF	1.160	1.054	1.068	1.222	1.149	1.223
Temperature/K	120	299	299	299	300	300
Coordination number	Na1: 6 Na2: 6	K1: 8 K2: 7	Rb1: 8 Rb1: 7	Rb1: 8 Rb2: 9	9	Cs1: 8 Cs2: 8
Coordination environment of M ⁺ ^b	Na1: 2S + 4O Na2: 2S + 4O	K1: 3S + 2N + 3O K2: 4S + 1N + 2O	Rb1: 3S + 2N + 3O Rb2: 4S + 1N + 2O	Rb1: 4S + 4O Rb2: 5S + 4O	7S + 2N	Cs1: 6S + 2N Cs2: 6S + 2N
H ₂ O/M ⁺	3	1	1	2	0	0
Dimensionality ^c	I ⁰ O ²	I ² O ¹	I ² O ¹	I ² O ¹	I ² O ¹	I ² O ¹
Polyhedra connectivity ^d	C ⁰ E ¹ F ⁰	K1: C ⁰ E ¹ F ² K2: C ¹ E ² F ¹	Rb1: C ⁰ E ¹ F ² Rb2: C ¹ E ² F ¹	Rb1: C ¹ E ⁰ F ² Rb2: C ¹ E ¹ F ¹	C ⁰ E ³ F ³	Cs1: C ⁰ E ⁴ F ⁰ Cs2: C ⁰ E ³ F ²

^a ttc is trithiocyanurate anion (C₃N₃S₃³⁻). ^b Coordination bond lengths are defined as ≤ 3.3 Å for Na-S, ≤ 2.5 Å for Na-N and Na-O, ≤ 3.7 Å for K-S, ≤ 3.2 Å for K-N and K-O, ≤ 3.9 Å for Rb-S, ≤ 3.4 Å for Rb-N and Rb-O, ≤ 4.1 Å for Cs-S, and ≤ 3.6 Å for Cs-N. ^c Inorganic connectivity, I^{*n*}, where M-X-M bonds extend the structure, and organic connectivity, O^{*m*}, where M-ligand-M extend the structure. ^d Numbers of corner sharing (C^{*x*}), edge sharing (E^{*y*}) and face sharing (F^{*z*}) polyhedra.

as clear light orange rhombohedral crystals and “Cs-TTC-2” as clear light orange plates.

Crystallographic data of all the alkali metal trithiocyanurates are summarized in Table 1 and their connectivities and coordination environments are compared in Fig. 2. The compositions were also confirmed by CHN analysis as described above. All the alkali metal trithiocyanurates contain a two-dimensional arrangement of trithiocyanurate monoanion (C₃N₃S₃H₂⁻ = ttcH₂⁻) building units, which is interleaved by alkali metal ion (M⁺) layers as illustrated in Fig. 3d. The most interesting feature of this system is the thiol-rich coordination environment formed around the alkali metal ions. Water molecules, where present, are always coordinated to a cation.

3.1.1 Coordination environment. Alkali metal ions are bound to S and N atoms of ttcH₂⁻ as well as oxygen atoms of H₂O. Apparently, with increasing size of alkali metal ions, the number of coordinated thio groups tends to increase from two to seven, while the number of coordinated water molecules tends to decrease from four to zero (Table 1). This observation is analogous to the situation found in alkaline earth carboxylates.^{26,27} These trends are explainable in terms of “hard and soft acids and bases”: the soft base of thioketone has a preference for bonding to the soft acid of the larger alkali metals, while the hard base of H₂O has a preference for the hard acid of the smaller alkali metals.

The thermogravimetric analyses (TGA) show that Na-TTC, and Rb-TTC-2, are dehydrated from room temperature, and that K-TTC, and Rb-TTC-1, are dehydrated above 100 °C (Fig. S1, ESI[†]). These results suggest that H₂O molecules are weakly bound to alkali metal ions in Na-TTC and Rb-TTC-2,

and more strongly in K-TTC and Rb-TTC-1. In addition, the amounts of water determined by TGA are consistent with those determined by X-ray diffraction: (i) 20.4 wt% loss for Na-TTC (52.2 g/Na⁺) corresponds to 2.9H₂O/Na⁺. This means that Na-TTC was fully dehydrated at 155 °C. The same holds true for the other two hydrated compounds. (ii) 7.3 wt% loss of K-TTC (17.0 g/K⁺) corresponds to 0.9H₂O/K⁺. (iii) 6.6 wt% loss of Rb-TTC-1 (18.5/Rb⁺) corresponds to 1.0H₂O/Rb⁺. (iv)

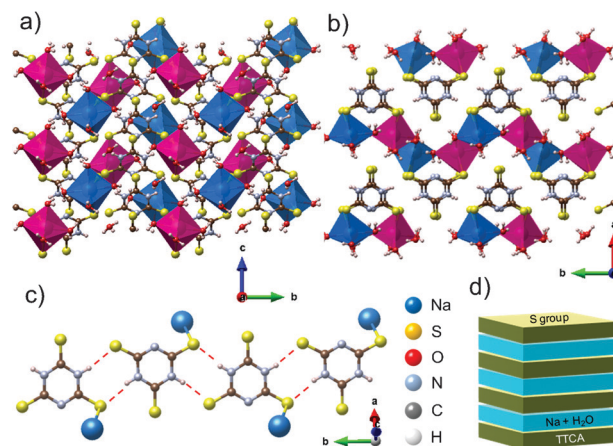


Fig. 3 Crystal structure of Na-TTC. (a) Na octahedra form dimers. Blue and red polyhedra represent the Na1 and Na2 coordination spheres, respectively. (b) Trithiocyanurates are stacked along the *c* axis and connect with each other through hydrogen bonding, as represented in panel ‘c’. (d) The organic layers are interleaved by the inorganic layers.

8.7 wt% loss of Rb-TTC-2 (31.0 g/Rb^+) corresponds to $1.7\text{H}_2\text{O/Rb}^+$ (supporting the presence of OH^-).

3.1.2 Dimensionality. The dimensionality of the hybrid systems is described in terms of both the inorganic connectivity, where metal–X–metal ($X = \text{O}, \text{N}$ or S) bonds extend the structure, and organic connectivity, where bonding through the ligands (metal–ligand–metal) extends the structure, as described in Cheetham *et al.*³ This is written in the shorthand I^nO^m where n is the inorganic dimensionality and m is the organic dimensionality, and their sum is the overall dimensionality of the framework. The dimensionalities of the alkaline metal trithiocyanurates are compared in Table 1.

Na-TTC has a two-dimensional structure (I^0O^2) formed by inorganic dimers (I^0) connected by the ligand molecules (O^2), as shown in Fig. 3a and 3b. The other structures are three-dimensional structures (I^2O^1) formed by inorganic sheets (I^2) connected by the ligand (O^1) (see Fig. 4–7).

3.1.3 Polyhedral connectivity. Coordination numbers of the alkali metal ions and connection between the polyhedra increase with size of alkali metal ions (Table 1). These trends reflect an increase of polyhedral condensation, or packing of metal ion polyhedra, with the size of metal ions.²⁶ The following paragraphs describe details of the structures.

In Na-TTC, Na ions are octahedrally coordinated by four H_2O molecules and two S-groups of different ttcH_2^{-1} ions (Fig. 2a, 3a and 3b and Table 1). The octahedra form isolated edge-sharing dimers in which the edges are H_2O molecules. The independent H_2O molecules having the O3 and O4 atoms (Fig. 2a) appear identical at room temperature (Fig. S5, ESI[†]), and the structure was determined in the space group $P2_1/c$ (Fig. S5 and Table S1, ESI[†]), but their hydrogen atom positions could not be refined without ambiguity. Thus, the

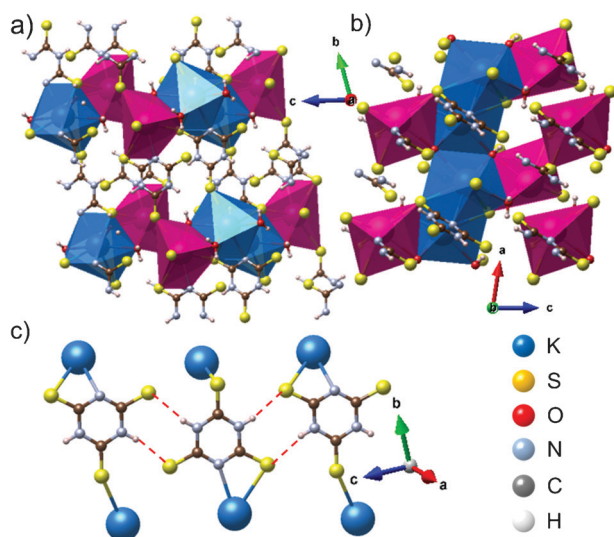


Fig. 4 Crystal structure of K-TTC, along the a axis (a) and the b axis (b). Blue and red polyhedra represent the K1 and K2 coordination spheres, respectively. (c) Hydrogen bonding network of trithiocyanurate anions. Rubidium trithiocyanurate hydrate, $\text{Rb}(\text{ttcH}_2)(\text{H}_2\text{O})$, “Rb-TTC-1”, is isostructural.

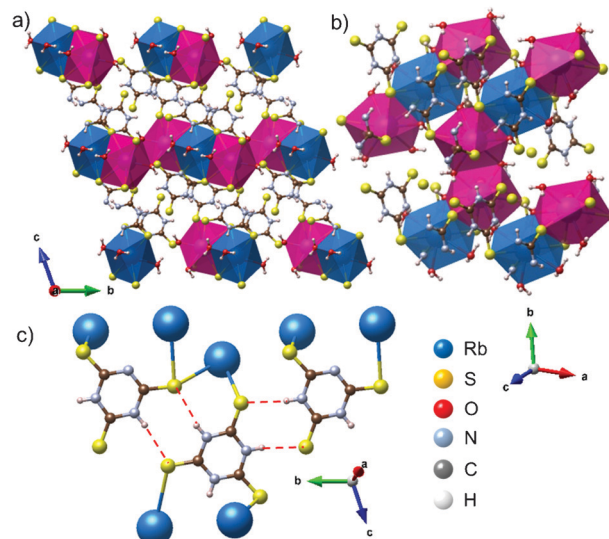


Fig. 5 Crystal structure of Rb-TTC-2, along the a axis (a) and the direction perpendicular to the inorganic layers (b). Blue and red polyhedra represent the Rb1 and Rb2 coordination spheres, respectively. (c) Hydrogen bonding network of trithiocyanurate anions.

structure of Na-TTC was also determined at 120 K (space group: $P2_1$), and O3 and O4 atoms were found to be independent in terms of hydrogen positions as well as two electron density peaks assignable to oxygen atoms.

In the isostructural compounds K-TTC and Rb-TTC-1, the inorganic sheets are formed by $\text{M}_2\text{--M}_1\text{--M}_1\text{--M}_2$ face-sharing tetramers, which are connected by edge sharing (Fig. 2b, 4a and 4b): $\text{M}_1\text{--M}_1$ shares a face formed by two

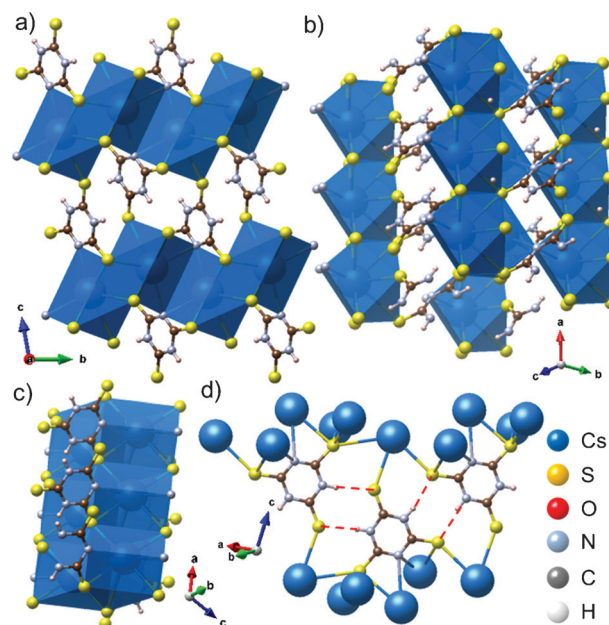


Fig. 6 Crystal structure of Cs-TTC-1. (a) The inorganic layers are interleaved by the organic layers along the c axis. Light blue polyhedra represent the Cs coordination spheres. (b, c) The face sharing polyhedral chains extend along the a axis. (d) Hydrogen bonding network of trithiocyanurate anions.

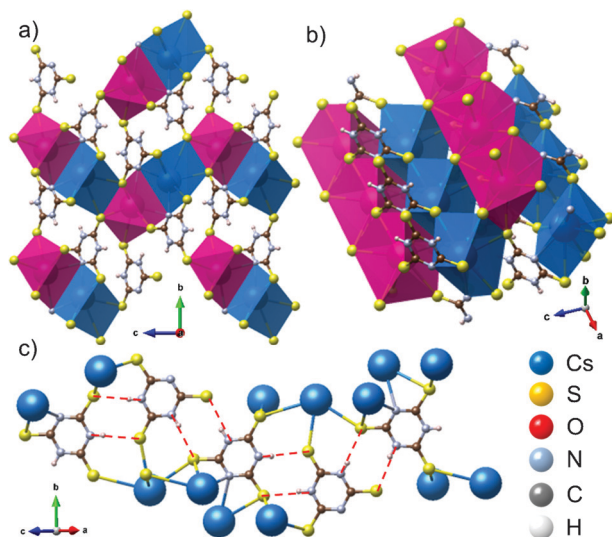


Fig. 7 Crystal structure of Cs-TTC-2. (a) The inorganic layers are interleaved by the organic layers along the *b* axis. Blue and red polyhedra represent the Cs1 and Cs2 coordination spheres, respectively. (b) The face sharing polyhedral chains (Cs2) extend along the *a* axis. These chains are connected to each other through the edge sharing polyhedral chains (Cs1) along the same direction. (c) Hydrogen bonding network of trithiocyanurate anions.

S-groups and two N-groups of two ttcH_2^- ions and an edge formed by two H_2O molecules, M1–M2 shares a face formed by one S-group and two H_2O molecules, and M2–M2 shares an edge formed by two S-groups. ttcH_2^- ions bridge two M^+ ions in the same inorganic layer as well as adjacent inorganic layers.

In Rb-TTC-2, the inorganic sheets are formed by Rb2–Rb1–Rb2 face-sharing trimers, which are connected by edge and corner sharing (Fig. 2c, 5a and 5b): Rb1–Rb2 shares a face formed by two S-groups and a H_2O molecule and a corner H_2O molecule, and Rb2–Rb2 shares an edge formed by two H_2O molecules. Interestingly, the Rb ions are coordinated by OH^- ions and neutral ttcH_3 molecules as well as ttcH_2^- ions and H_2O molecules (Fig. 2c), where the OH^- ions exist as two H_2O molecules sharing one proton (H3). The neutral ttcH_3 molecules and ttcH_2^- ions bridge two Rb ions in the same inorganic layer as well as adjacent inorganic layers.

In Cs-TTC-1 (Fig. 2d and 6a–6c), the inorganic sheets consist of Cs polyhedral chains formed by face sharing. Cs ions share a face formed by three S-groups as well as an edge formed by two N-groups. In Cs-TTC-2 (Fig. 2e, 7a and 7b), the inorganic sheets consist of polyhedral chains formed by face sharing of Cs2 ions, and these are connected by edge sharing with Cs1 ions. Cs2–Cs2 shares a face formed by three S-groups, Cs1–Cs2 shares an edge formed by two N-groups or an edge formed by two S-groups, and Cs1–Cs1 shares an edge formed by two S-groups. In these Cs compounds, ttcH_2^- ions bridge several Cs ions in the same inorganic layer as well as adjacent inorganic layers (Fig. 6d and 7c).

3.1.4 Hydrogen bonding between ttcH_2^- ions. The ttcH_2^- layers are formed by hydrogen bonding of ttcH_2^- ions in

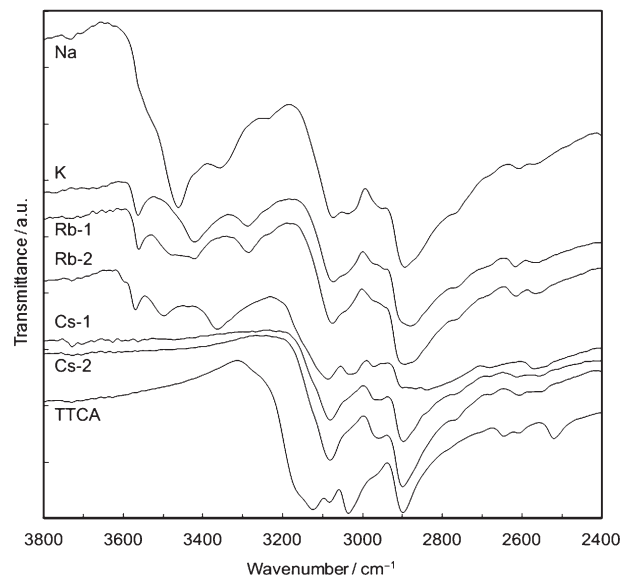


Fig. 8 FTIR spectra of alkali metal trithiocyanurates of Na-TTC, K-TTC, Rb-TTC-1, Rb-TTC-2, Cs-TTC-1 and Cs-TTC-2 in comparison to the spectrum of pure trithiocyanuric acid.

three different types: type 1, Na-TTC, K-TTC and Rb-TTC-1 have one-dimensional linear hydrogen-bonding networks, where one S-group and one N-group at opposite sides of ttcH_2^- are not involved (Fig. 3c and 4c). Type 2, Rb-TTC-2 and Cs-TTC-1 have one-dimensional zig-zag hydrogen-bonding networks, where one S-group and one N-group at adjacent positions are not involved (Fig. 5c and 6d). Type 3, Cs-TTC-2 has one-dimensional wavy hydrogen-bonding networks, where ttcH_2^- molecules are connected alternately by type 1 and type 2 systems (Fig. 7c).

In the FTIR spectrum of the trithiocyanuric acid (Fig. 8 and S3, ESI†), N–H stretching bands ($2800\text{--}2250\text{ cm}^{-1}$) are dominant for X–H stretching ($X = \text{N}, \text{S}$ and O), while weak S–H stretching bands ($2500\text{--}2700\text{ cm}^{-1}$) are also observed.²⁵ Thus, some of ttcH_3 molecules are in the thiol form (Scheme 1). In hybrid crystals, the S–H bands are weak but still observable, suggesting that a small portion of protons move from N–H sites through hydrogen bonding to S–H sites. They also exhibit O–H stretching bands ($3200\text{--}3700\text{ cm}^{-1}$), except for the anhydrous Cs-TTC polymorphs. This result is consistent with the hydrogen positions determined by X-ray diffraction. Details are described in the ESI† file.

3.2 Ionic conductivity

Using single crystals, ionic conductivities were measured by the AC impedance method. The impedance spectrum of K-TTC was typical for solid-state ion conductors: a semicircle in the higher frequency region and a tilted vertical line in the lower frequency region, as shown in Fig. 9.²⁸ Because the data were obtained for a single crystal sample, the semicircle can be simply attributed to a bulk phenomenon, not

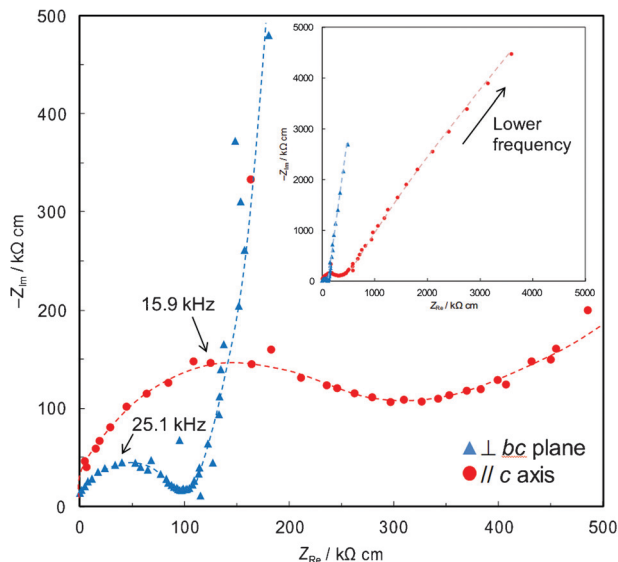


Fig. 9 Complex-plane impedance plots of single crystal K-TTC at 25 °C in air. The *ac* facet was placed in contact with microelectrodes patterned on a SiO₂ substrate. AC impedance spectra in two different directions (perpendicular to the *ab* plane and parallel to the *c* axis) were measured. AC amplitude: 100 mV. Frequency range: 1 MHz to 1 Hz. The dashed lines are for better visualization of the spectra.

to grain boundaries. Thus, we calculated conductivity values from the diameters of these semicircles.

The ionic conductivity values of K-TTC under atmospheric conditions (25 ± 0.2 °C) were 1.1 × 10⁻⁵ S cm⁻¹ in the direction perpendicular to the *bc* plane and 3.1 × 10⁻⁶ S cm⁻¹ along the *c* axis. These values are comparable to those of classic solid-state ion conductors (10⁻³ to 10⁻⁸ S cm⁻¹).²⁹ These materials reversibly became insulators on heating or under nitrogen flow; that is, the ionic conduction appeared to be related to humidity.

The compounds Na-TTC, Cs-TTC-1 and Cs-TTC-2 were insulators even in air, while Rb-TTC-2 exhibited a modest conductivity of 3.3 × 10⁻⁷ S cm⁻¹ along the [3 -1 0] direction under ambient conditions at 25 °C (Fig. S6, ESI†). Regarding Rb-TTC-1, a flat facet large enough for the measurements could not be found. The conductivity values of K-TTC showed some variation among different single crystals; for example, one crystal exhibited ionic conductivities of 3.6 × 10⁻⁶ S cm⁻¹ (25 ± 0.2 °C) at the direction perpendicular to the *bc* plane and 2.3 × 10⁻⁷ S cm⁻¹ along the *c* axis, even in humid air (these conductivities were 10⁴ times lower in ambient air).

It is clear that these systems are proton conductors. Regarding the mechanism of the ionic conductivity, we propose two possibilities: in one mechanism, K-TTC is conductive without H₂O deficient sites in the structures. Crystallographically, the occupancy of the water molecules in K-TTC is 100% at ambient conditions. In view of the coordination environments (Table 1), only these isostructural compounds have polyhedra formed by coordination with S-groups, N-groups and O-groups. In particular, the coordination with the anionic N-group of ttCH₂⁻¹ is unique among the hydrated structures. Within a K2 coordination sphere (see Fig. 2b), protons may diffuse

from H₂O molecules (O1) through S5 atoms and N1 atoms to S4 atoms (O1–S5 = 3.21 Å, S5–N1 = S4–N1 = 2.64 Å). Since these distances are close to S–N hydrogen bonding distance, 3.27–3.32 Å, such proton diffusion is considered to be reasonable.

As discussed above, S4 atoms and S5 atoms form hydrogen bonding with N-groups of different ttCH₂⁻ ions, which transports protons between different coordination spheres as indicated by the IR spectra. Within the K1 coordination spheres, similar proton diffusion can be considered (O1–S6 = 3.25 Å). In view of the decrease of ionic conductivity at higher temperature or in nitrogen atmosphere, the possible intrinsic H₂O deficiency is considered to inhibit proton diffusion through this mechanism.

In an alternative mechanism, the ionic conductivity might originate from oxonium ions which may be formed by moisture. Similar humidity dependence was reported for proton conduction of classic proton conductive crystals. According to the literature, the stoichiometry and conductivity of intrinsic conductors (e.g., CsHSO₄ 10⁻² S cm⁻¹ at 150 °C)³⁰ are almost humidity independent, while those of surface conductors, where gel-like domains are formed between rigid frameworks by hydration, depend strongly on humidity.³¹ Thus, the ion conduction mechanism of K-TTC could be surface conduction. Since the mechanical properties of hybrid systems are, in general, weaker than those of classic solid-state materials (e.g., oxides), the variation of conductivity values might reflect the importance of extrinsic crystal defects in hybrid systems' ionic conductivity.

4 Conclusions

Six novel hybrid crystals of alkali metal trithiocyanurates, Na(ttCH₂)(H₂O)₃, K(ttCH₂)(H₂O), Rb(ttCH₂)(H₂O), Rb₃(ttCH₂)₂(ttCH₃)₂(H₂O)₅(OH), and two anhydrous polymorphs of Cs(ttCH₂) were synthesized and their structures were determined by single crystal X-ray diffraction. Their ionic conductivities were measured by single crystal AC impedance methods, and K(ttCH₂)(H₂O) exhibited proton conductivity comparable to those of classic solid-state ion conductors. The conductivity may be attributed to ion diffusion through coordination spheres, or to hydration of defects. In order to confirm the mechanism, further detailed investigations are needed.

Acknowledgements

This work was supported by an Advanced Investigator Award from the European Research Council (ERC) and the World Premier International Research Center Initiative on “Materials Nanoarchitectonics (WPI-MANA)” from MEXT, Japan. The authors thank the MANA foundry (NIMS) for the experimental support on the preparation of the microelectrodes.

Notes and references

- 1 *Solid State Electrochemistry*, ed. P. G. Bruce, Cambridge University Press, Cambridge, 1995.

- 2 *Proton Conductors*, ed. P. Colomban, Cambridge University Press, Cambridge, 1992.
- 3 A. K. Cheetham, C. N. R. Rao and R. K. Feller, *Chem. Commun.*, 2006, 4780–4795.
- 4 B. A. Zhou, Y. Imai, A. Kobayashi, Z. M. Wang and H. Kobayashi, *Angew. Chem., Int. Ed.*, 2011, **50**, 11441–11445.
- 5 A. K. Cheetham, C. N. R. Rao and R. K. Feller, *Chem. Commun.*, 2006, 4780–4795.
- 6 A. K. Cheetham and C. N. R. Rao, *Science*, 2007, **318**, 58–59.
- 7 A. Thirumurugan and A. K. Cheetham, *Eur. J. Inorg. Chem.*, 2010, 3823–3828.
- 8 M. Armand, S. Grugeon, H. Vezin, S. Laruelle, P. Ribiere, P. Poizot and J. M. Tarascon, *Nat. Mater.*, 2009, **8**, 120–125.
- 9 J. A. Hurd, R. Vaidhyanathan, V. Thangadurai, C. I. Ratcliffe, I. L. Moudrakovski and G. K. H. Shimizu, *Nat. Chem.*, 2009, **1**, 705–710.
- 10 S. Bureekaew, S. Horike, M. Higuchi, M. Mizuno, T. Kawamura, D. Tanaka, N. Yanai and S. Kitagawa, *Nat. Mater.*, 2009, **8**, 831–836.
- 11 D. Umeyama, S. Horike, M. Inukai, Y. Hijikata and S. Kitagawa, *Angew. Chem., Int. Ed.*, 2011, **50**, 11706–11709.
- 12 D. Umeyama, S. Horike, M. Inukai, T. Itakura and S. Kitagawa, *J. Am. Chem. Soc.*, 2012, **134**, 12780–12785.
- 13 T. Yamada, M. Sadakiyo and H. Kitagawa, *J. Am. Chem. Soc.*, 2009, **131**, 3144–3145.
- 14 P. Kopel, K. Dolezal, L. Machala and V. Langer, *Polyhedron*, 2007, **26**, 1583–1589.
- 15 K. R. Henke, A. R. Hutchison, M. K. Krepps, S. Parkin and D. A. Atwood, *Inorg. Chem.*, 2001, **40**, 4443–4447.
- 16 P. A. W. Dean, M. Jennings, T. M. Houle, D. C. Craig, I. G. Dance, J. M. Hook and M. L. Scudder, *CrystEngComm*, 2004, **6**, 543–548.
- 17 S. Ahn, J. PrakashaReddy, B. M. Kariuki, S. Chatterjee, A. Ranganathan, V. R. Pedireddi, C. N. R. Rao and K. D. M. Harris, *Chem.–Eur. J.*, 2005, **11**, 2433–2439.
- 18 *Proton Conductors: Solids, Membranes and Gels (Materials and Devices)*, ed. P. Colomban, Cambridge University Press, Cambridge, 1992.
- 19 S. Tominaka, N. Akiyama, F. Croce, T. Momma, B. Scrosati and T. Osaka, *J. Power Sources*, 2008, **185**, 656–663.
- 20 G. M. Sheldrick, *Acta Crystallogr., Sect. A: Found. Crystallogr.*, 2008, **64**, 112–122.
- 21 O. V. Dolomanov, L. J. Bourhis, R. J. Gildea, J. A. K. Howard and H. Puschmann, *J. Appl. Crystallogr.*, 2009, **42**, 339–341.
- 22 A. G. Csaszar, G. Czako, T. Furtenbacher, J. Tennyson, V. Szalay, S. V. Shirin, N. F. Zobov and O. L. Polyansky, *J. Chem. Phys.*, 2005, **122**, 21430501–21430510.
- 23 K. Momma and F. Izumi, *J. Appl. Crystallogr.*, 2011, **44**, 1272–1276.
- 24 S. Tominaka, *J. Mater. Chem.*, 2011, **21**, 9725–9730.
- 25 D. H. Williams and I. Fleming, *Spectroscopic Methods in Organic Chemistry*, McGraw-Hill Publishing Company, Berkshire, England, 1997.
- 26 E. H. Falcão, Naraso, R. K. Feller, G. Wu, F. Wudl and A. K. Cheetham, *Inorg. Chem.*, 2008, **47**, 8336–8342.
- 27 L. N. Appelhans, M. Kosa, A. V. Radha, P. Simoncic, A. Navrotsky, M. Parrinello and A. K. Cheetham, *J. Am. Chem. Soc.*, 2009, **131**, 15375–15386.
- 28 R. D. Armstrong and M. Todd, in *Solid State Electrochemistry*, ed. P. G. Bruce, Cambridge University Press, Cambridge, 1995, pp. 264–291.
- 29 P. Colomban and A. Novak, in *Proton Conductors: Solids, Membranes and Gels (Materials and Devices)*, ed. P. Colomban, Cambridge University Press, Cambridge, 1992, pp. 38–60.
- 30 A. Potier, in *Proton Conductors: Solids, Membranes and Gels (Materials and Devices)*, ed. P. Colomban, Cambridge University Press, Cambridge, 1992, pp. 1–17.
- 31 P. Colomban and A. Novak, in *Proton Conductors: Solids, Membranes and Gels (Materials and Devices)*, ed. P. Colomban, Cambridge University Press, Cambridge, 1992, pp. 61–78.